Marine Geophysical Researches (2006) 27:129–136
DOI 10.1007/s11001-005-0266-y

Coastal bathymetry from hyperspectral remote sensing data: comparisons with high resolution multibeam bathymetry

Michelle L. McIntyre[1,*], David F. Naar[1], Kendall L. Carder[1], Brian T. Donahue[1] and David J. Mallinson[2]
[1]*College of Marine Science, University of South Florida, 140 7th Avenue South, St. Petersburg, FL, 33701, USA;* [2]*Department of Geology, East Carolina University, Greenville, USA;* *Author for correspondence *(Phone +1-727-553-3336; E-mail: mcintyre@marine.usf.edu)*

Received 3 November 2004, accepted 23 June 2005

Key words: hyperspectral, bathymetry, optics

Abstract

We present a large-scale quantitative test of a hyperspectral remote-sensing reflectance algorithm. We show that coastal bathymetry can be adequately derived through model inversions using data from the Airborne Visible-Infrared Imaging Spectrometer instrument. Data are analyzed from a shore-perpendicular transect 5 km offshore Sarasota, Florida at water depths ranging from 10 m to 15.5 m. Derived bottom depths are compared to a high-resolution multibeam bathymetry survey. Model-derived depths are biased 4.9% shallower than the mean of the multibeam depths with an RMS error of 7.83%. These results suggest that the model performs well for retrieving bottom depths from hyperspectral data in subtropical coastal areas in water depths ranging from 10 m to 15.5 m.

Introduction

There is growing interest in applying optical remote sensing techniques to obtain bathymetry in shallow water marine environments (Lyzenga, 1985; Clark, 1987; O'Neil et al., 1989; Philpot, 1989). However, the use of satellite sensors in shallow waters is complicated by the combined atmospheric, water, and bottom signals (Jerlov, 1976). This includes variations due to water column scattering and absorption due to dissolved and suspended materials such as sediments, chlorophyll, and colored dissolved organic mater. The introduction of high-resolution multispectral sensors has allowed the light reflected from the seafloor to be spectrally deconvolved and used to extract benthic information (Bierwirth et al., 1993; Werdell and Roesler, 2003). However, in many cases, these methods require the input of known depth values (Lyzenga, 1978), or assumptions of homogenous seafloor properties (Philpot, 1989).

The use of airborne hyperspectral sensors provides the spatial and spectral resolution necessary to investigate complex coastal environments (Mustard et al., 2001). Additionally, the models used to extract information from remotely sensed data are continually evolving to be more effective in unmixing the optical signal to accurately estimate bottom depths (Gordon and Brown, 1974; Mobley et al., 1993; Lee et al., 1994; Maritorena et al., 1994). One method for evaluating bottom depths from remotely sensed spectra is by developing a spectral library representative of end-member properties that is used to compare measured and modeled spectra (Louchard et al., 2003). Although this method is useful, simulations must be recomputed when the water optical properties change. Another method for evaluating hyperspectral data is through inverse modeling of the radiative transfer function (Durand et al., 2000). This approach allows simultaneous derivations of optical properties through an iterative curve-fitting process with a minimization scheme. The inversion modeling approach has shown promising results in shallow marine waters (Lee et al., 1999).

The objective of this study was to present the first large-scale quantitative test of a hyperspectral remote-sensing reflectance model in deriving bottom depths in a shallow water marine environment by comparing model-derived depths to high-resolution multibeam bathymetry data. The model tested here was developed by Lee et al. (2001) for

simultaneously deriving inherent optical properties and seafloor properties from remotely sensed data. The model minimizes the difference between modeled and measured spectra by adjusting values of absorption, backscattering, bottom albedo, and bottom depth. The model-derived depths have been shown to agree well at depths of 0–4.6 m, when compared with NOAA bathymetry charts (Lee et al., 2001), however these charts are based on low-resolution bathymetric data collected more than 20 years prior to collection of the hyperspectral data. Additionally, comparisons between the charts and derived depths have only been qualitative, by comparing scanned bathymetry charts. Therefore, more quantitative comparisons between high-resolution data sets collected concurrently are needed to fully test the model. In this paper we use high-resolution multibeam bathymetry data to test model-derived depths from airborne hyperspectral data.

Methods

Hyperspectral imagery

The Airborne Visible-Infrared Imaging Spectrometer (AVIRIS) instrument, an Earth-observing imaging spectrometer funded by the National Aeronautics and Space Administration and built by the Jet Propulsion Laboratory, is flown aboard a NASA ER-2 airplane at a nominal altitude of 20 km (Vane et al., 1993). The scanner is a whisk-broom imager that sweeps back and forth, producing images of upwelling radiance in 224 spectral channels from 400 to 2400 nm with a 20×20 m spatial resolution. The images produced are 614 pixels across-track and collected in 512 line sets, with each pixel representing 400 m^2. The AVIRIS data used in this study were collected near the western coast of Florida offshore of the city of Sarasota (Figure 1). The Sarasota AVIRIS data, covering an area of approximately 200 km^2, was collected on May 21, 1999 at 1425 to 1429 (GMT) from 27°14.7′ N to 27°21.3′ N and 82°40.5′ W to 82°48′ W, with a solar zenith angle of 40.8 degrees.

The AVIRIS data were vicariously calibrated following the methods of Carder et al. (1993), corrected for atmospheric effects, and then inverted using the method of Lee et al. (2001) to derive bottom depth. The imagery was geo-rectified using a set of ground-control points collected in-flight.

Bathymetry data

The inner box in Figure 1 indicates the extent of the ground-truth multibeam bathymetry data used

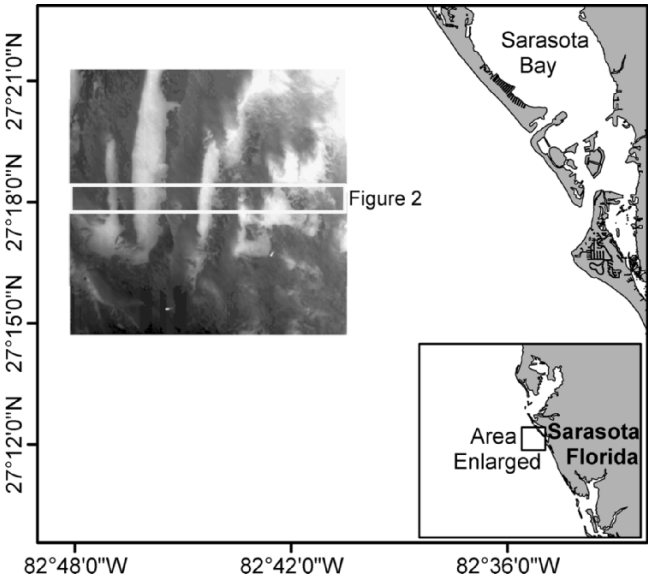

Figure 1. Airborne Visible-Infrared Imaging Spectrometer (AVIRIS) data at 550 nm used in this analysis. Bright areas indicate high optical reflectance and dark areas represent low optical reflectance. Note that this image has been contrast-enhanced. Inset map in the SE corner of the map indicates the location of imagery data collected offshore of Sarasota, Florida. The rectangular box within the imagery indicates the extent of high-resolution multibeam bathymetry data and denotes the extent of Figure 2.

in this study. The multibeam bathymetry survey, collected July 7–9, 2000, covered an area of approximately 20 km^2 that extended from 27°17′ N to 27°19′ N and 82°38′ W to 82°48′ W. These data were collected using the University of South Florida's Kongsberg Simrad EM 3000 multibeam system. The 300 kHz system acquires high-resolution bathymetry data with a swath width of 130 degrees, which in shallow water gives a swath width of four times the water depth. The system generates 127 beams using a sonar pulse of 0.15 ms at a maximum ping rate of 25 Hz (Naar et al., 1999).

The multibeam bathymetry data were processed and corrected for errors in position, tidal changes, and sound velocity fluctuations caused by temperature and salinity differences throughout the water column. Both the AVIRIS-derived depths and ground-truth multibeam depths were corrected to mean sea level. The tide level during the AVIRIS over flight was measured at the nearby Mote Marine Laboratory in Sarasota, Florida. The tide levels during the multibeam bathymetry data collection were generated with a circulation model developed for the West Florida Shelf (He and Weisberg, 2003). The computed tide level compared well with the measured tide, however, due to the location of Mote Marine Lab's tidal gauge inside Sarasota Bay, the magnitude of the measured tide was less than the computed tide at the study location offshore. However, the tidal difference was less than 0.3 m. The tidal range during the multibeam survey was less than 0.5 m. The high-resolution multibeam bathymetry data were resampled to the resolution of the AVIRIS data, for purposes of direct comparison.

A comparison among three repeated multibeam bathymetry surveys collected within a 9-month period show minimal changes in the bathymetry of the study area (McIntyre et al., 2002; McIntyre, 2003). Therefore, although there is a temporal gap between the AVIRIS over flight and the multibeam survey, the multibeam bathymetry data are not expected to show significant departures from the bottom configuration at the time of the AVIRIS over flight.

Results and observations

Multibeam bathymetry

Measured depths range from 10.0 to 15.35 m (Figure 2a). The multibeam bathymetry data (Figure 2a) show the seafloor is composed of two

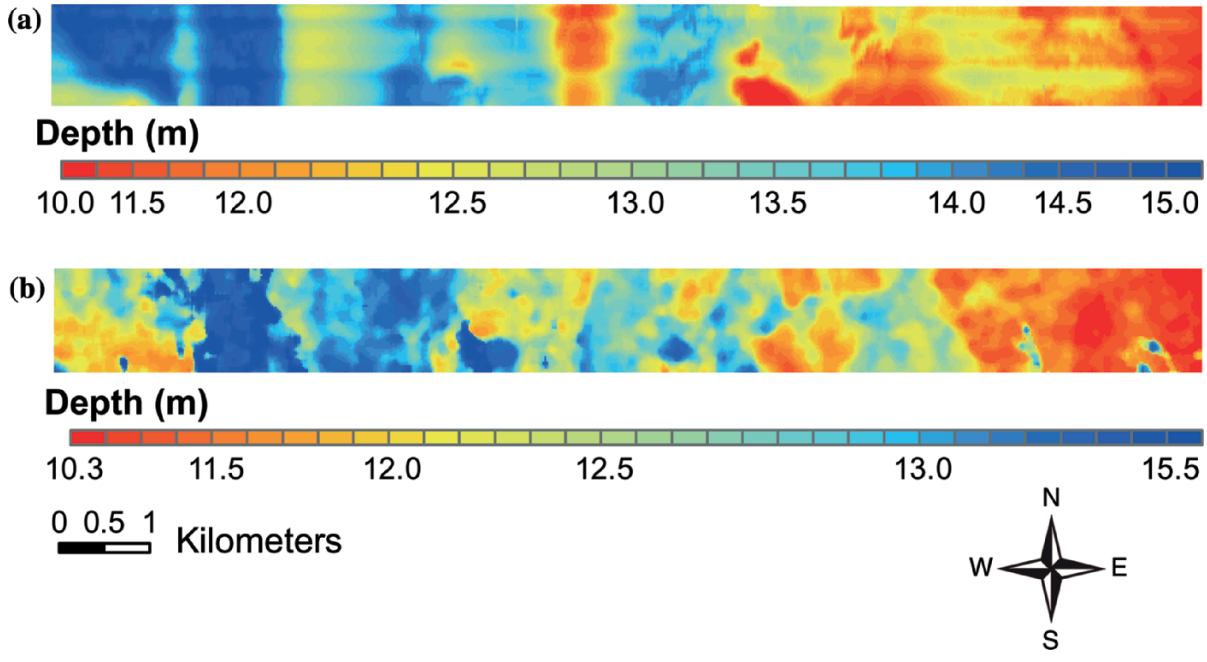

Figure 2. (a) Image of multibeam bathymetry data, using Mean Sea Level datum. (b) Image of AVIRIS-derived bottom depths.

general bathymetric provinces; nearshore (10–12.5 m) and offshore (12.5–15.5 m). The nearshore area is shaped by irregular, discontinuous features. Offshore (west) of the 12 m isobath, however, these features become more distinct, regular, and oriented north to south.

AVIRIS depths

Figure 2b shows the image of AVIRIS-derived bottom depths, ranging from 10.23 to 15.33 m. The image of derived depths shows a general correspondence with multibeam bathymetry. The ranges in depth between the AVIRIS and multibeam depths are similar, however, the easternmost and westernmost 2 km of AVIRIS data appear shallower than multibeam depths. A comparison of the measured multibeam bathymetry with the AVIRIS-derived depths (Figure 3) shows that most modeled depths are shallower than measured depths. The difference between AVIRIS and multibeam depths ranges from 0 to 3.3 m with a mean difference of 0.9 m.

The error in AVIRIS-derived depths was quantified by calculating the percent error as follows:

$$\text{Percent Error} = \frac{100[\text{Depth(m)}_{\text{Multibeam}} - \text{Depth(m)}_{\text{AVIRIS}}]}{\text{Depth(m)}_{\text{Multibeam}}}$$

Where the percent error is negative, the modeled depths are deeper than measured depths and are overestimated by the model. Where the percent error is positive the modeled depths are shallower than measured depths and are underestimated by the model. The percent error in AVIRIS-derived bottom depths ranges from −12.1% to 21.73%, with a mean error of 4.9% and RMS of 7.83% (Figure 4). A comparison of percent error and multibeam depths shows the AVIRIS-derived depths are consistently and increasingly underestimated in water depths greater than 14 m (Figure 5). At depths greater than 14 m ($n = 5973$) the mean error is 12.1%, RMS error is 12.9%, and mean difference in depth is 1.8 m, however at depths less than 14 m ($n = 28{,}456$) the mean error is 3.4%, RMS error is 7.14% and mean difference in depth is 0.67 m. (Figure 5). Profiles of multibeam bathymetry and percent error (Figure 6) show the magnitude of error inversely follows the morphology of the seafloor. The AVIRIS depths are underestimated (shallower) near the troughs in bathymetry and overestimated (deeper than measured depths) near the peaks.

The AVIRIS depths were corrected by using a site-specific algorithm to relate the mean error in AVIRIS depths to the measured depths. The following empirical second-order polynomial describes the mean error in AVIRIS depths:

$$y = -0.100715x^2 + 3.23972x - 11.5607$$

where x is the model-derived AVIRIS depth ($r = 0.8$). When the mean error is removed from AVIRIS depths the corrected depths have an error

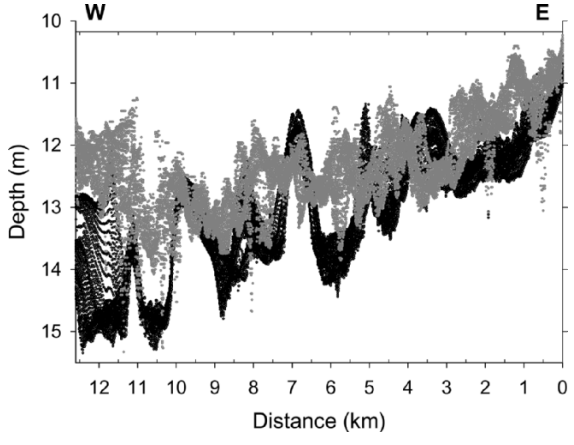

Figure 3. Profiles multibeam bathymetry depths (black points) and AVIRIS-derived depths (gray points). The study area, as represented in Figure 2, consists of 115 east-west profiles, all of which are shown here.

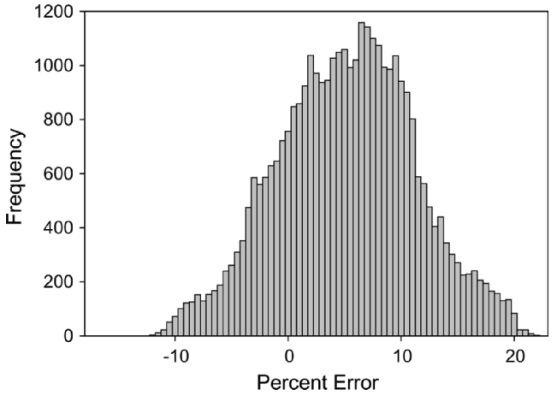

Figure 4. Histogram of percent error in AVIRIS-derived depths. Negative values of percent error occur where AVIRIS-derived depths are too deep relative to multibeam depths, and positive values of percent error occur where AVIRIS-derived depths are too shallow relative to multibeam depths.

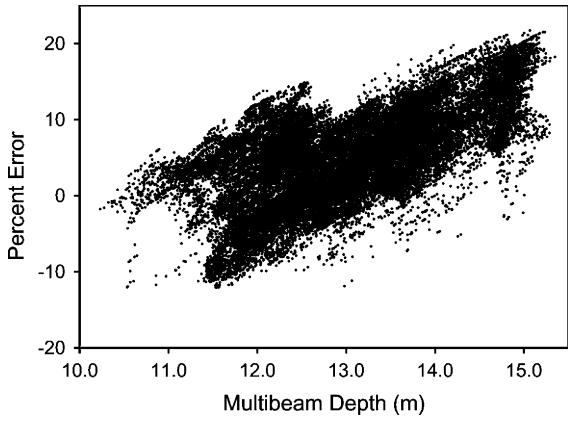

Figure 5. Comparison of percent error in AVIRIS-derived depths and multibeam depths. Negative values of percent error occur where AVIRIS-derived depths are too deep relative to multibeam depths, and positive values of percent error occur where AVIRIS-derived depths are too shallow relative to multibeam depths.

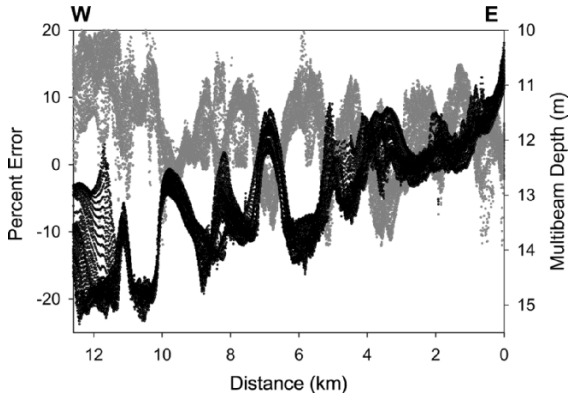

Figure 6. Profiles of percent error in AVIRIS-derived depths (gray points) and multibeam depths (black points). The study area, as represented in Figure 2, consists of 115 east–west profiles, all of which are shown here.

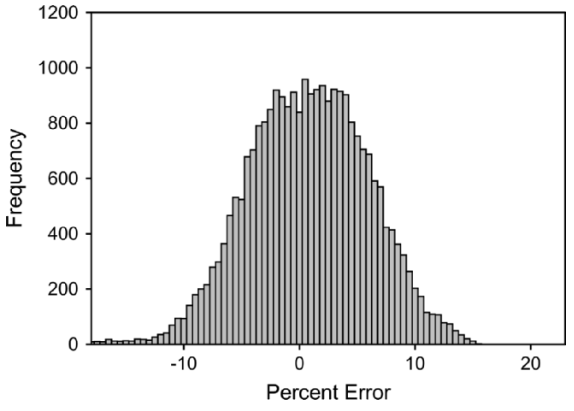

Figure 7. Histogram of percent error in bias-corrected AVIRIS-derived depths. Negative values of percent error occur where AVIRIS-derived depths are too deep relative to multibeam depths, and positive values of percent error occur where AVIRIS-derived depths are too shallow relative to multibeam depths.

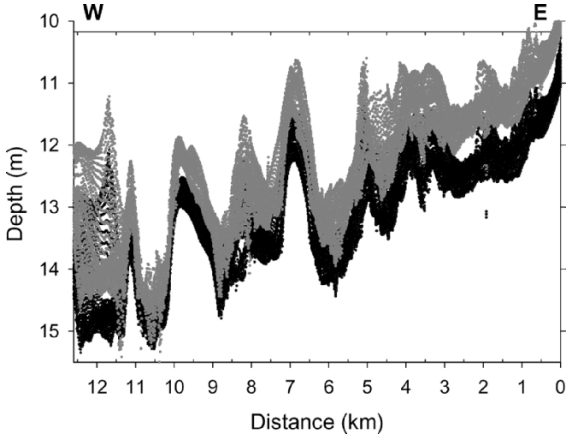

Figure 8. Profiles multibeam bathymetry depths (black points) and corrected AVIRIS-derived depths (gray points). The study area, as represented in Figure 2, consists of 115 east-west profiles, all of which are shown here.

range of −6% to 8.4% and RMS error of 5.6% (Figure 7) and show a good correspondence with multibeam depth (Figure 8). At depths greater than 14 m, corrected AVIRIS depths agree with measured depths within 7.4%.

Discussion

The large errors in AVIRIS depths may arise from two main factors: measurement errors arising from the airborne sensor, and derivation errors arising from model limitations and assumptions. The AVIRIS sensor was initially designed for terrestrial applications with target reflectances of 20–50%, however water reflectances are normally less than 5% (Carder et al., 1993). Additionally, as water depth increases the amount of light reflected back to the sensor from the bottom is diminished. Therefore, the signal-to-noise ratio of the sensor is important when extracting useful information from a weak bottom signal. The signal-to-noise ratio of the AVIRIS sensor has been continually improved throughout its flight history. After the flight season of 1999, the sensor underwent substantial upgrades that improved signal-to-noise ratio and reduced data artifacts noted during flight seasons 1987–1999 (Eastwood et al., 2000).

The second factor contributing to errors in the AVIRIS depths is the derivation errors caused by model assumptions. The model assumes the spectral shape of the bottom albedo is known, allowing only the magnitude of albedo to change from pixel to pixel. At the time these model depths were derived only two spectral shapes were used for the derivations. However, the bottom albedo shape has been shown to deviate from the typical sand and seagrass spectra used in the model (McIntyre, 2003). An expanded albedo database from *in situ* measurements is needed and may improve model derivations. Additional error may be introduced by the influence of bottom slopes on the reflectance. The model assumes the bottom is horizontal so that the reflected radiance is independent of the incident and observational angles. Carder et al. (2003) found that this model slightly underestimates depths for bright bottom facets that face the sun whereas shaded facets produce overestimates of depth. However, bottom facets throughout the study area are significantly less than 2 degrees and therefore, this assumption introduces less than 5% error in the modeled depths. In addition to errors arising from model assumptions, Zhan et al. (2003) notes that local optimization methods such as the model used here (Lee et al., 2001) are prone to becoming trapped in local solution and may not necessarily converge to a global solution. This may compromise the results of the retrievals and produce erroneous data. In this study, the Lee et al. (2001) inversion method may have produced a bottom depth for a given reflectance using an optimization function that did not fully converge to the global optima.

The model performed most accurately between 10 m and 14 m (Figure 5). On average the model underestimated depths by 4.9%. The largest errors in derived depths occurred in the deepest portion of the study area where depths were greater than 14 m (westernmost 2 km). Here the model underestimated depths by as much as 21%. The reason for this is due to the limitations of remote sensing of water depth. The fundamental principle of remotely sensing water depth is that light will penetrate the water column and reflect off the seafloor back to the sensor. However, the depth of penetration is dependent on turbidity, suspended sediments, phytoplankton, and dissolved organic compounds because they act to scatter and absorb light (Green, 1996). These effects, in addition to increasing water depth and bottom absorption, will increase the contribution of water-reflected light relative to bottom-reflected light, thereby decreasing the influence of the bottom reflection on the above-water spectra (Carder et al., 2003). The question of what percentage of bottom contribution is required for an accurate depth estimate is currently under investigation by the authors.

Hyperspectral remote sensing of bottom depths has been shown to achieve results within 10% at water depths ranging from 0 to 4.6 m (Lee et al., 2001). Additionally, Sandidge and Holyer (1998) show that by employing a neural network, depths can be reasonably estimated at water depths of 0–6 m. The work presented here shows that water depths can be adequately derived from hyperspectral remote sensing data in water depths of 10–14 m. Below 14 m, derived depths are underestimated by $>12\%$ on average due to the natural limitations of optical remote sensing. However, we show here that a simple empirically derived algorithm can be used to correct the model-derived bathymetry. This algorithm was specific to the data collected at this location, but this method could prove useful for correcting remotely sensed water depths at other locations provided an adequate amount of ground truth data are available for validating the derived depths.

Summary and conclusions

This study was conducted as part of the Hyperspectral Coupled Ocean Dynamics Experiments, supported by the Office of Naval Research. Our objective was to test the performance of optical models in deconvolving the optical signal over shallow-water environments. In this paper we present, for the first time, a large-scale quantitative test of the hyperspectral model developed by Lee et al. (2001) for deriving bottom depth over a large shallow-water environment ranging from 10 to 15.5 m water depth in the subtropical waters of the eastern Gulf of Mexico. The results show the model is sufficient in deriving bottom depths with an RMS error of 7.83%, and full error range of −12.1 to 22.73%, using more than 34,000-point comparisons. Modeled depths agree well with measured depths from 10 to 14 m. Below 14 m the modeled depths are underestimated

due to depth limitations of the remotely sensed data. However, these data can be corrected using a simple site-specific, empirically derived model. These results indicate the model is robust in deriving shallow water bathymetry in water depths ranging from 10 to 15.5 m. Improvements such as an expanded spectral library of bottom albedo, and increased signal-to-noise ratio will become a valuable tool in deriving bottom depths from hyperspectral remote sensing data.

Acknowledgments

Financial support was provided by the Office of Naval Research through N00014-96-1-5032, N00014-99-1-0787, and N00014-02-1-0636. The authors thank Dr. Robert Chen for AVIRIS data preparation, and ONR Program Manager Joan Cleveland. M. McIntyre is grateful for the assistance and comments from Dr. Peter Howd, during his service on her Master's committee.

References

Bierwirth, P.N., Lee, T.J. and Burne, R.V., 1993, Shallow seafloor reflectance and water depth derived by unmixing multispectral imagery, *Photogramm. Eng. Rem. S.* **59**, 331–338.

Carder, K.L., Reinersman, P., Chen, R.F. and Muller-Karger, F.E., 1993, AVIRIS calibration and application in coastal oceanic environments, *Remote Sens. Environ.* **44**, 205–216.

Carder, K.L., Liu, C., Lee, Z.P., English, D.C., Patten, J., Chen, R.F. and Ivey, J.E., 2003, Illumination and turbidity effects on observing faceted bottom elements with uniform lambertian albedos, *Limnol. Oceanogr.* **48**, 355–363.

Clark, R.K., Fay, T.H. and Walker, C.L., 1987, Bathymetry calculations with Landsat 4 TM imagery under a generalized ratio assumption, *Appl. Optics* **26**, 4036–4038.

Durand, D., Bijaoui, J. and Cauneau, F., 2000, Optical remote sensing of shallow-water environmental parameters: A feasibility study, *Remote Sens. Environ.* **73**, 152–161.

Eastwood, M.L., Green, R.O., Sarture, C.M., Chippindale, B.J., Chovit, C.J., Faust, J.A., Johnson, D.L., Monacos, S.P. and Raney, J., 2000, Recent improvements to the AVIRIS sensor: Flight season 2000. *in*: Proceedings of the Tenth Annual JPL Airborne Geoscience Workshop, Pasadena, California.

Green, E.P., Mumby, P.J., Edwards, A.J. and Clark, C.D., 1996, A review of remote sensing for the assessment and management of tropical coastal resources, *Coast. Manage.* **24**, 1–40.

Gordon, H.R. and Brown, O., 1974, Influence of bottom depth and albedo on the diffuse reflectance of a flat homogeneous ocean, *Appl. Optics* **13**, 2153–2159.

He, R. and Weisberg, R.H., 2003, West Florida shelf circulation and temperature budget for the 1998 fall transition, *Cont. Shelf Res.* **23**, 777–800.

Jerlov, N.G., 1976, *Marine Optics*. New York: Elsevier.

Lee, Z., Carder, K.L., Hawes, S.K., Steward, R.G., Peacock, T.G. and Davis, C.O., 1994, Model for the interpretation of hyperspectral remote-sensing reflectance, *Appl. Optics* **33**, 5721–5732.

Lee, Z., Carder, K.L., Mobley, C.D., Steward, R.G. and Patch, J.S., 1999, Hyperspectral remote sensing for shallow waters II. Deriving bottom depths and water properties by optimization, *Appl. Optics* **38**, 3831–3843.

Lee, Z., Carder, K.L., Chen, R.F. and Peacock, T.G., 2001, Properties of the water column and bottom derived from AVIRIS data, *J. Geophys. Res.* **106**, 11639–11651.

Louchard, E., Reid, P.R., Stephens, F.C., Davis, C.O., Leathers, R.A. and Downes, T.V., 2003, Optical remote sensing of benthic habitats and bathymetry in coastal environments at Lee Stocking Island, Bahamas: A comparative spectral classification approach, *Limnol. Oceanogra.* **48**, 511–521.

Lyzenga, D.R., 1978, Passive remote sensing techniques for mapping water depth and bottom features, *Appl. Optics* **17**, 379–383.

Lyzenga, D.R., 1985, Shallow-water bathymetry using combined Lidar and passive multispectral scanner data, *Int. J. Remote Sen.* **6**, 115–125.

Maritorena, R.J., Morel, A. and Gentilli, B., 1994, Diffuse reflectance of oceanic shallow waters: Influence of water depth and bottom albedo, *Limnol. Oceanogr.* **39**, 1689–1703.

McIntyre, M.L., Naar, D.F., Carder, K.L., Howd, P.A., Lewis, J.M., Donahue, B.T. and Chen, R.F., 2002, Comparison of bathymetry and bottom characteristics from hyperspectral remote sensing data and shipborne acoustic measurements. *in*: Eos Transactions of the American Geophysical Union Fall Meeting Supplements, 6–10 December 2002, p. 47. San Francisco, California.

McIntyre, M.L., 2003, *Testing a model for deriving bathymetry from airborne hyperspectral data by comparing with multibeam sonar data. MS thesis*. St. Petersburg, Florida: University of South Florida.

Mobley, C.D., 1993, Comparison of numerical models for computing underwater light fields, *Appl. Optics* **32**, 7484–75041.

Mustard, J.F., Staid, M.I. and Fripp, W.J., 2001, A semianalytical approach to the calibration of AVIRIS data to reflectance over water application in a temperate estuary, *Remote Sens. Environ.* **75**, 335–349.

Naar, D.F., Donahue, B.T., DeWitt, N., Farmer, A.S., Jarrett, B., Palmsten, M., Reynolds, B.J. and Wilder, D., 1999, Preliminary results from a EM 3000 multibeam class survey along the west coast of the Florida carbonate platform. *in*: Eos Transactions of the American Geophysical Union Fall Meeting Supplements, 13–17 December 1999, p 46. San Francisco, California.

O'Neill, N.T. and Miller, J.R., 1989, On calibration of passive optical bathymetry through depth soundings analysis and treatment of errors resulting from the spatial variation of environmental parameters, *Int. J. Remote Sen.* **10**, 1481–1501.

Philpot, W.D., 1989, Bathymetric mapping with passive multispectral imagery, *Appl. Optics* **28**, 1569–1578.

Sandidge, J.C. and Holyer, R.J., 1998, Coastal bathymetry from hyperspectral observations of water radiance, *Remote Sens. Environ.* **65**, 341–352.

Vane, G., Green, R.O., Chrien, T.G., Enmark, H.T., Hansen, E.G. and Porter, W.M., 1993, The Airborne Visible/Infrared Imaging Spectrometer (AVIRIS), *Remote Sens. Environ.* **44**, 127–143.

Werdell, P.J. and Roesler, C.S., 2003, Remote assessment of benthic substrate composition in shallow waters using multispectral reflectance, *Limnol. Oceanogr.* **48**(1, part 2), 557–567.

Zhan, H, Lee, Z.P., Shi, P., Chen, C. and Carder, K.L., 2003, Retrieval of water optical properties for optically deep waters using genetic algorithms, *IEEE T. Geosci. Remote Sens.* **41**, 1123–1128.